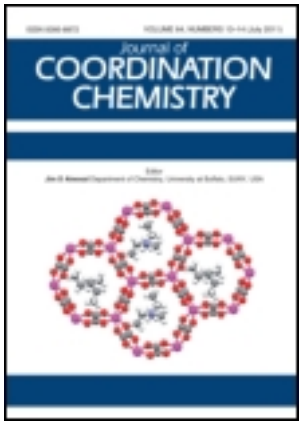

Journal of Coordination Chemistry
Publication details, including instructions for authors and subscription information:
http://www.tandfonline.com/loi/gcoo20

Ruthenium(II) complexes: synthesis, cytotoxicity in vitro, apoptosis, DNA-binding, photocleavage, and antioxidant activity studies

Zhen-Hua Liang [a], Zheng-Zheng Li [a], Hong-Liang Huang [b] & Yun-Jun Liu [a]

[a] School of Pharmacy, Guangdong Pharmaceutical University, Guangzhou 510006, P.R. China

[b] School of Life Science and Biopharmaceutical, Guangdong Pharmaceutical University, Guangzhou 510006, P.R. China

Published online: 22 Sep 2011.

To cite this article: Zhen-Hua Liang, Zheng-Zheng Li, Hong-Liang Huang & Yun-Jun Liu (2011) Ruthenium(II) complexes: synthesis, cytotoxicity in vitro, apoptosis, DNA-binding, photocleavage, and antioxidant activity studies, Journal of Coordination Chemistry, 64:19, 3342-3352, DOI: 10.1080/00958972.2011.619533

To link to this article: http://dx.doi.org/10.1080/00958972.2011.619533

Journal of Coordination Chemistry
Vol. 64, No. 19, 10 October 2011, 3342–3352

Ruthenium(II) complexes: synthesis, cytotoxicity *in vitro*, apoptosis, DNA-binding, photocleavage, and antioxidant activity studies

ZHEN-HUA LIANG†, ZHENG-ZHENG LI†,
HONG-LIANG HUANG‡* and YUN-JUN LIU†*

†School of Pharmacy, Guangdong Pharmaceutical University,
Guangzhou 510006, P.R. China
‡School of Life Science and Biopharmaceutical, Guangdong Pharmaceutical University,
Guangzhou 510006, P.R. China

(*Received 15 June 2011; in final form 22 August 2011*)

Two new ruthenium(II) complexes, $[Ru(dmp)_2(APIP)](ClO_4)_2$ (**1**) (APIP = 2-(2-aminophenyl imidazo[4,5-*f*][1,10]phenanthroline), dmp = 2,9-dimethyl-1,10-phenanthroline) and $[Ru(dmp)_2(HAPIP)](ClO_4)_2$ (**2**) (HAPIP = 2-(2-hydroxyl-5-aminophenyl)imidazo[4,5-f][1,10]phenanthroline), were synthesized and characterized. The DNA-binding properties of these complexes were investigated by absorption titration, viscosity measurements, and photoactivated cleavage. The DNA-binding constants for **1** and **2** have been determined to be $2.3\ (\pm 0.3) \times 10^4\ (\text{mol L}^{-1})^{-1}$ and $3.3\ (\pm 0.4) \times 10^4\ (\text{mol L}^{-1})^{-1}$. The results indicate that **1** and **2** interact with DNA through intercalative mode. The cytotoxicities of **1** and **2** were assessed against BEL-7402, HepG-2 and MCF-7 cell lines using standard MTT assay. The apoptosis induced by these complexes was studied with the acridine orange/ethidium bromide staining method. The antioxidant activity on hydroxyl radical was also investigated.

Keywords: Ruthenium(II) complexes; Cytotoxicity; Apoptosis; Antioxidant activity; DNA binding

1. Introduction

The interaction of transition metal complexes with DNA has attracted much attention [1] with studies showing that small molecules bind to DNA by electrostatic binding, groove binding, and intercalative binding. Generally, the intercalating ligand should contain an aromatic heterocycle that can insert and stack between the base pairs of double helical DNA [1]. Some ruthenium(II) complexes exhibit unique characteristics, $[Ru(bpy)_2(ppd)]^{2+}$ shows no luminescence in aqueous solution at ambient temperature, but luminesces brightly upon binding intercalatively with pdd between adjacent DNA base pairs, displaying the characteristic of a ''molecular light switch'' [2]. Ruthenium(II) complexes can bind to DNA through intercalation or groove binding [3–6].

*Corresponding authors. Email: honglianghuangcn@hotmail.com; lyjche@163.com

Journal of Coordination Chemistry
ISSN 0095-8972 print/ISSN 1029-0389 online © 2011 Taylor & Francis
http://dx.doi.org/10.1080/00958972.2011.619533

Intercalation, a strongly favorable binding mode, involves the π-stacking of a ligand between the adjacent base pairs of DNA, requiring the intercalative ligand to be a flat, extended aromatic system.

Progress on ruthenium complexes as antitumor drugs has been made; $[Ru(bpy)_2(bfipH)]^{2+}$ can effectively induce the apoptosis of HeLa cells [7], *mer*-$[RuCl_3(DMSO)(H_2biim)]$ shows high anti-metastatic effects (DMSO = dimethyl sulfoxide and H_2biim = 2,2′-biimidazole) [8]. $[Ru(bpy)_2(dppn)]^{2+}$ can effectively inhibit proliferation of MCF-7 cells with a low IC_{50} ($3 \pm 1\ \mu mol\ L^{-1}$) [9]. The antiproliferative mechanism of $[Ru(phen)_2(DNPIP)]^{2+}$ on BEL-7402 and Hepg-2 are G2/M and S phase arrest, respectively [10]. In this article, we report synthesis and DNA binding of two new ruthenium(II) complexes, $[Ru(dmp)_2(APIP)]^{2+}$ (**1**) (dmp = 2,9-dimethyl-1,10-phenanthroline, APIP = 2-(2-aminophenyl)imidazo[4,5-*f*][1,10]phenanthroline) and $[Ru(dmp)_2(HAPIP)]^{2+}$ (**2**) (HAPIP = (2-(2-hydroxyl-5-aminophenyl)imidazo[4,5-*f*][1,10]phenanthroline, scheme 1). The cytotoxicities of the two complexes were evaluated using the MTT method. The apoptosis and antioxidant activities induced by these complexes were also investigated.

2. Experimental

2.1. *Materials and methods*

Calf thymus DNA (CT-DNA) was obtained from the Sino-American Biotechnology Company. pBR322 DNA was obtained from Shanghai Sangon Biological Engineering & Services Co., Ltd. pGL 3 plasmid DNA was obtained from Promega (USA). DMSO and RPMI 1640 were purchased from Sigma. Cell lines of hepatocellular (BEL-7402), hepatocellular (HepG-2), and breast cancer (MCF-7) were purchased from American Type Culture Collection; agarose and ethidium bromide (EB) were obtained from Aldrich. $RuCl_3 \cdot 3H_2O$ was purchased from Kunming Institution of Precious Metals. 1,10-Phenanthroline was obtained from Guangzhou Chemical Reagent Factory. Doubly distilled water was used to prepare buffers (5 mmol L^{-1} tris(hydroxymethylaminomethane)-HCl, 50 mmol L^{-1} NaCl, pH = 7.2). A solution of CT-DNA in the buffer gave a ratio of UV absorbance at 260 and 280 nm of *ca* 1.8–1.9:1, indicating that the DNA was sufficiently free of protein [11]. The DNA concentration per nucleotide was determined by absorption spectroscopy using the molar absorption coefficient (6600 $(mol\ L^{-1})^{-1}\ cm^{-1}$) at 260 nm [12].

Microanalysis (C, H, and N) was carried out with a Perkin-Elmer 240Q elemental analyzer. Electrospray mass spectra (ES-MS) were recorded on an LCQ system (Finnigan MAT, USA) using methanol as mobile phase. The spray voltage, tube lens offset, capillary voltage, and capillary temperature were set at 4.50 KV, 30.00 V, 23.00 V and 200°C, respectively, and the quoted m/z values are for the major peaks in the isotope distribution. ^1H NMR spectra were recorded on a Varian-500 spectrometer. All chemical shifts were given relative to tetramethylsilane (TMS). UV-Vis spectra were recorded on a Shimadzu UV-3101PC spectrophotometer and emission spectra were recorded on a Shimadzu RF-4500 luminescence spectrometer at room temperature.

2.2. *Synthesis of 1 and 2*

2.2.1. Synthesis of $[Ru(dmp)_2(APIP)](ClO_4)_2$ (1). A mixture of $[Ru(dmp)_2Cl_2]\cdot 2H_2O$ (0.312 g, 0.5 mmol) [13], NPIP (0.171 g, 0.05 mmol) [NPIP = (2-(2-aminophenyl)imidazo[4,5-*f*][1,10]phenanthroline)] [14], and ethanol (25 cm^3) were refluxed under argon for 8 h to give a clear red solution. Upon cooling, a red precipitate was obtained by dropwise addition of saturated aqueous $NaClO_4$ solution. The crude product was purified by column chromatography on neutral alumina with CH_3CN-toluene (3 : 1, v/v) as eluent. The main red band was collected. The solvent was removed under reduced pressure and a red powder obtained. The red powder was dissolved in ethanol (30 cm^3). Pd/C (0.20 g, 10% Pd) and $NH_2NH_2\cdot H_2O$ (8 cm^3) were added in the above solution and refluxed under argon for 8 h to give a clear red solution. $[Ru(dmp)_2(APIP)](ClO_4)_2$ was obtained with the same method described for the red powder. Yield: 72%. Anal. Calcd for $C_{47}H_{37}N_9Cl_2O_8Ru$: C, 54.92; H, 3.63; N, 12.26. Found (%): C, 54.55; H, 3.67; N, 12.53. ES-MS [CH_3CN, *m*/*z*]: 827.3 ($[M–2ClO_4–H]^+$), 414.9 ($[M–2ClO_4]^{2+}$). ^1H NMR (500 MHz, DMSO-d_6): δ 8.91 (d, 2 H, $J = 8.5$ Hz), 8.43 (dd, 4 H, $J = 8.5$ Hz), 8.24 (d, 2 H, $J = 8.6$ Hz), 7.98 (d, 4 H, $J = 8.5$ Hz), 7.37 (d, 4 H, $J = 8.5$ Hz), 7.18 (d, 2 H, $J = 8.0$ Hz), 7.05 (d, 1 H, $J = 7.0$ Hz), 6.77 (d, 2 H, $J = 8.0$ Hz), 6.59 (t, 1 H, $J = 7.0$ Hz), 3.38 (s, 2 H, H_{NH2}), 2.50 (s, 12 H, H_{CH3}).

2.2.2. Synthesis of $[Ru(dmp)_2(HAPIP)](ClO_4)_2$ (2). A mixture of *cis*-$[Ru(dmp)_2Cl_2]\cdot 2H_2O$ [13] (0.312 g, 0.5 mmol) and HAPIP (0.164 g, 0.5 mmol) [15] in ethanol (30 cm^3) was refluxed under argon for 8 h to give a clear red solution. Upon cooling, a red precipitate was obtained by dropwise addition of saturated aqueous $NaClO_4$ solution. The crude product was purified by column chromatography on neutral alumina with CH_3CN-toluene (3 : 1, v/v) as eluent. The main red band was collected. The solvent was removed under reduced pressure and a red powder obtained. Yield: 72%. Anal. Calcd for $C_{47}H_{37}N_9Cl_2O_9Ru$: C, 54.08; H, 3.57; N, 12.08. Found (%): C, 53.97; H, 3.62; N, 12.34. ES-MS [CH_3CN, *m*/*z*]: 843.5 ($[M–2ClO_4–H]^+$), 422.6 ($[M–2ClO_4]^{2+}$). ^1H NMR (500 MHz, DMSO-d_6): δ 8.92 (d, 2 H, $J = 8.0$ Hz), 8.72 (dd, 4 H, $J = 8.5$ Hz), 8.23 (d, 2 H, $J = 8.5$ Hz), 7.98 (dd, 4 H, $J = 8.5$ Hz), 7.46 (d, 2 H, $J = 7.5$ Hz), 7.37 (d, 4 H, $J = 8.5$ Hz), 7.22 (d, 1 H, $J = 4.5$ Hz), 6.69 (d, 1 H, $J = 5.5$ Hz), 6.57 (t, 1 H, $J = 5.0$ Hz), 4.57 (s, 1 H, H_{OH}), 3.36 (s, 2 H, H_{NH2}), 2.48 (s, 12 H, H_{CH3}).

Caution: Perchlorate salts of metal compounds with organic ligands are potentially explosive, and only small amounts of the material should be prepared and handled with great care.

2.3. *DNA-binding and photoactivated cleavage*

The DNA-binding and photoactivated cleavage experiments were performed at room temperature. Buffer A [5 mmol L^{-1} tris(hydroxymethyl)aminomethane (tris) hydrochloride, 50 mmol L^{-1} NaCl, pH 7.0] was used for absorption titration, luminescence titration, and viscosity measurements. Buffer B (50 mmol L^{-1} Tris-HCl, 18 mmol L^{-1} NaCl, pH 7.2) was used for DNA photocleavage experiments.

Viscosity measurements were carried out using an Ubbelodhe viscometer maintained at a constant temperature at 25.0 (±0.1)°C in a thermostatic bath. DNA samples about

200 bp in average length were prepared by sonication to minimize complexities arising from DNA flexibility [16]. Flow time was measured with a digital stopwatch, and each sample was measured three times, and an average flow time was calculated. Relative viscosities for DNA in the presence and absence of complexes were calculated from the relation $\eta = (t - t^0)/t^0$, where t is the observed flow time of the DNA-containing solution and t^0 is the flow time of buffer alone [17, 18]. Data are presented as $(\eta/\eta_0)^{1/3}$ *versus* binding ratio [19], where η is the viscosity of DNA in the presence of complexes and η_0 is the viscosity of DNA alone.

Absorption titrations of the complex in buffer were performed using a fixed concentration (20 μmol L^{-1}) of complex to which increments of the DNA stock solution were added. Ru-DNA solutions were incubated for 5 minbefore the absorption spectra were recorded. The intrinsic binding constants K, based on the absorption titration, were measured by monitoring the changes in absorption at the metal-to-ligand transfer (MLCT) band with increasing concentration of DNA using the following equation [20],

$$\frac{[\mathrm{DNA}]}{\varepsilon_a - \varepsilon_f} = \frac{[\mathrm{DNA}]}{\varepsilon_b - \varepsilon_f} + \frac{1}{K_b(\varepsilon_b - \varepsilon_f)}, \quad (1)$$

where [DNA] is the concentration of DNA in base pairs, ε_a, ε_f, and ε_b correspond to the apparent absorption coefficient A_{obsd}/[Ru], the extinction coefficient for the free ruthenium complex and the extinction coefficient for the ruthenium complex in the fully bound form, respectively. In plots of [DNA]/(ε_a–ε_f) *versus* [DNA], K_b is given by the ratio of slope to the intercept.

For the gel electrophoresis experiment, supercoiled pBR322 DNA (0.1 μg) was treated with the Ru(II) complexes in buffer B, and the solution was then irradiated at room temperature with a UV lamp (365 nm, 10 W). The samples were analyzed by electrophoresis for 1.5 h at 80 V on a 0.8% agarose gel in TBE (89 mmol L^{-1} tris-borate acid, 2 mmol L^{-1} EDTA, pH = 8.3). The gel was stained with 1 μg mL^{-1} EB and photographed on an Alpha Innotech IS–5500 fluorescence chemiluminescence and visible imaging system.

2.4. *Continuous variation analysis*

Binding stoichiometries were obtained for **1** and **2** with CT-DNA using the method of continuous variation [21]. The concentrations of both complex and DNA were varied, while the sum of the reactant concentrations was kept constant at 50 μmol L^{-1} (in terms of base pairs for the DNA). Solutions of complexes and DNA were prepared in tris-HCl buffer (pH = 7.4). In the sample solutions, the mole fraction χ of complex varied from 0 to 1.0 in 0.1 ratio steps. The fluorescence intensities of these mixtures were measured at 25°C using an excitation wavelength of 460 nm. The intensity in fluorescence was plotted *versus* the mole fraction χ of complex to generate a Job plot. Linear regression analysis of the data was performed with the software Origin 7.0.

2.5. *Cell culture and cytotoxicity assay* in vitro

Standard 3-(4,5-dimethylthiazole)-2,5-diphenyltetrazolium bromide (MTT) assay procedures were used [22]. Cells were placed in 96-well microassay culture plates

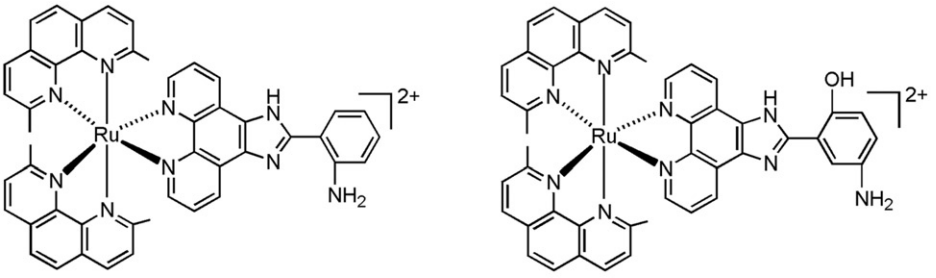

1 2

Scheme 1. The structures of **1** and **2**.

(8×10^3 cells per well) and grown overnight at 37°C in a 5% CO_2 incubator. The complexes tested were dissolved in DMSO and diluted with RPMI 1640 and then added to the wells to achieve final concentrations ranging from 10^{-6} to 10^{-4} mol L^{-1}. Control wells were prepared by addition of culture medium (100 μL). Wells containing culture medium without cells were used as blanks, and cisplatin was used as positive control. The plates were incubated at 37°C in a 5% CO_2 incubator for 72 h. Upon completion of the incubation, stock MTT dye solution (20 μL, 5 mg mL^{-1}) was added to each well. After 4 h, buffer (100 μL) containing DMF (50%) and sodium dodecyl sulfate (20%) was added to solubilize the MTT formazan. The optical density of each well was then measured on a microplate spectrophotometer at a wavelength of 490 nm. The IC_{50} values were determined by plotting the percentage viability *versus* concentration on a logarithmic graph and reading off the concentration at which 50% of cells remain viable relative to the control. Each experiment was repeated three times to get the mean values. Three different tumor cell lines were the subjects of this study: BEL-7402, HepG-2, and MCF-7.

2.6. *Apoptosis assessment by acridine orange/EB staining*

Apoptosis studies were performed with a staining method utilizing acridine orange (AO) and EB [23]. According to the difference in membrane integrity between necrotic and apoptosis, AO can pass through cell membrane, but EB cannot. Under fluorescence microscope, living cells appear green, necrotic cells stain red but have a nuclear morphology resembling that of viable cells, apoptosis cells appear green, and morphological changes such as cell blebbing and formation of apoptotic bodies will be observed. A monolayer of BEL-7402 cells was incubated in the absence or presence of **1** (25 μmol L^{-1}) at 37°C and 5% CO_2 for 48 h. Then each cell culture was stained with AO/EB solution (100 μg · mL^{-1} AO, 100 μg · mL^{-1} EB). Samples were observed under a fluorescence microscope.

2.7. *Antioxidant activity against hydroxyl radical*

The hydroxyl radical (•OH) in aqueous media was generated by the Fenton system [24]. Solutions of the tested complexes were prepared with DMF. The assay mixture (5 mL)

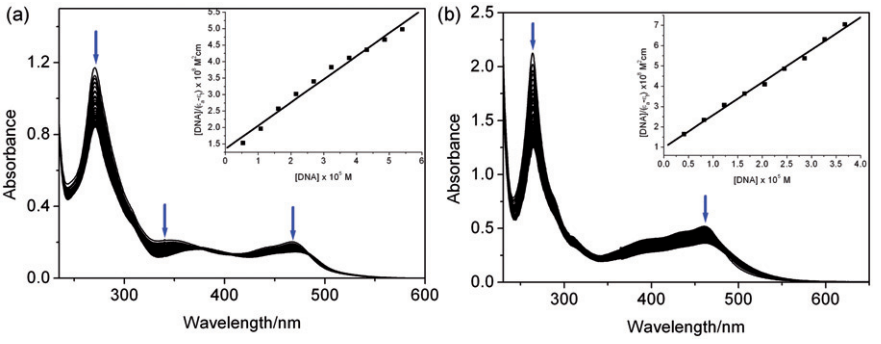

Figure 1. Absorption spectra of **1** (a) and **2** (b) in Tris-HCl buffer upon addition of increasing concentrations of CT-DNA. [Ru] = 20 μmol L^{-1}. Arrow shows the absorbance change with increasing DNA concentration. The insets are plots of [DNA]/($\varepsilon_a - \varepsilon_f$) *vs.* [DNA] for the titration of DNA with Ru(II) complexes.

contained: safranin (28.5 μmol L^{-1}), EDTA-Fe(II) (100 μmol L^{-1}), H_2O_2 (44.0 μmol L^{-1}), the tested compounds (0.5–4.5 μmol L^{-1}) and a phosphate buffer (67 mmol L^{-1}, pH = 7.4). The assay mixtures were incubated at 37°C for 30 min in a water bath and the absorbance measured at 520 nm. All the tests were run in triplicate and expressed as the mean. A_i is the absorbance in the presence of the tested compound; A_0 is the absorbance in the absence of tested compounds; A_c is the absorbance in the absence of tested compound, EDTA-Fe(II), H_2O_2. The suppression ratio (η_a) was calculated on the basis of $(A_i - A_0)/(A_c - A_0) \times 100\%$.

3. Results and discussion

3.1. *Electronic absorption titration*

The UV-Vis absorption spectra of **1** and **2** in the absence and presence of CT-DNA are illustrated in figure 1. Upon successive addition of DNA, absorptions at 460 and 459 nm for **1** and **2** underwent sharp decrease in intensities with hypochromisms as defined by $H\% = 100\ (A_{free} - A_{bound})/A_{free}$, being 26.41% and 35.03%. The large hypochromism values indicate that **1** and **2** strongly bind to CT-DNA. In order to compare the DNA-binding strength quantitatively, the intrinsic DNA-binding constants K_b are derived by monitoring the changes in absorbance at MLCT bands, giving K_b of 2.3 (±0.3) × 10^4 and 3.3 (±0.4) × 10^4 $(mol\,L^{-1})^{-1}$. These values are comparable to $[Ru(bpy)_2(hnip)]^{2+}$ [4.2 (±0.2) × 10^4 $(mol\,L^{-1})^{-1}$] [6] and $[Ru(dmb)_2(ITAP)]^{2+}$ [4.5 (±0.3) × 10^4 $(mol\,L^{-1})^{-1}$] [25], which are smaller than those previously reported for DNA intercalators [15].

3.2. *Luminescence studies and continuous variation analysis*

Changes in emission intensities of **1** and **2** in aqueous solution with increasing DNA concentrations are shown in figure 2. As DNA concentration increases, an obvious enhancement in emission intensity is observed. The emission intensities of **1** and **2**

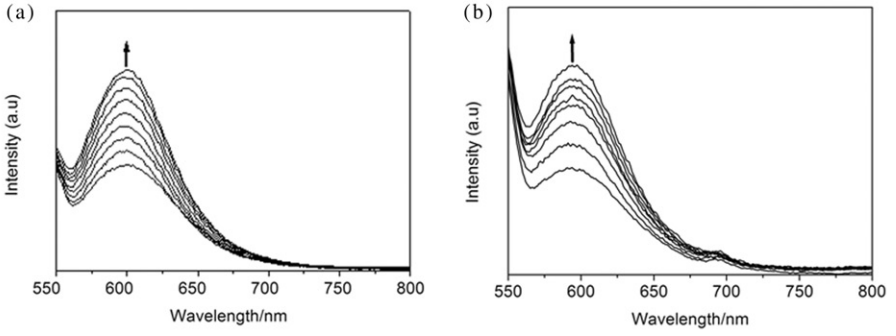

Figure 2. Emission spectra of **1** (a) and **2** (b) in Tris-HCl buffer in the absence and presence of CT-DNA. Arrow shows the intensity change upon increasing DNA concentrations.

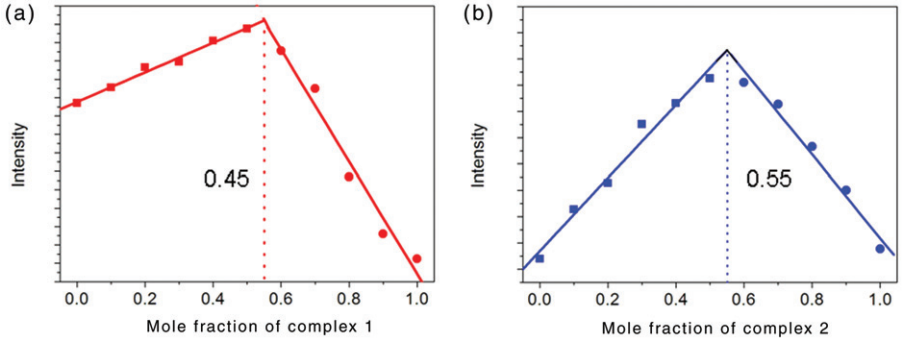

Figure 3. Job plot using luminescence data for **1** (a) and **2** (b) with CT-DNA in Tris-HCl buffer, pH = 7.0.

increase to 1.44 and 1.89 times the original intensities, respectively. Binding stoichiometry with CT-DNA was investigated by luminescence-based Job plot (figure 3). Major inflection points for **1** and **2** at 0.54 and 0.55 were observed, consistent with a 1 : 1 [complex]/[DNA] binding mode.

3.3. *Viscosity measurements*

Optical photophysical probes provide necessary, but not sufficient, clues to support a binding model. Hydrodynamic measurements that are sensitive to length change (i.e., viscosity and sedimentation) are regarded as the least ambiguous and most critical tests of a binding model in solution in the absence of crystallographic structural data [16, 26]. To provide key evidence for DNA-binding mode of these complexes, viscosity measurements were carried out. Usually, intercalation requires that the DNA helix lengths are separated to accommodate the binding ligand, leading to an increase in DNA viscosity. Figure 4 shows the changes in viscosity upon addition of **1** and **2**. On increasing the amounts of **1** and **2**, the relative viscosities of CT-DNA solution increase steadily. The increased viscosity, which may depend on affinity to DNA, follows the order **1** < **2**. These results suggest that **1** and **2** intercalate between base pairs of DNA or participate in groove binding.

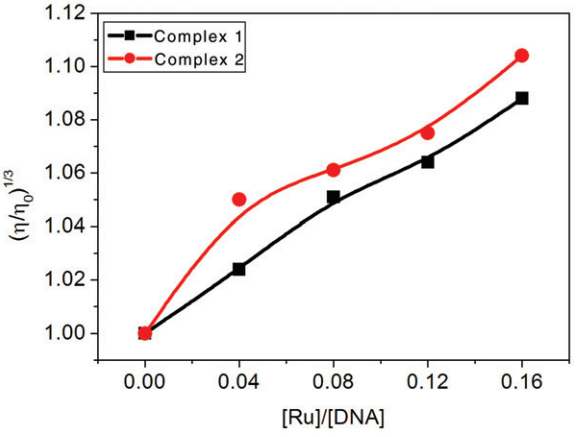

Figure 4. Effect of increasing amounts of **1** (■) and **2** (•) on the relative viscosity of CT-DNA at 25 (±0.1)°C. [DNA] = 0.25 mmol L^{-1}.

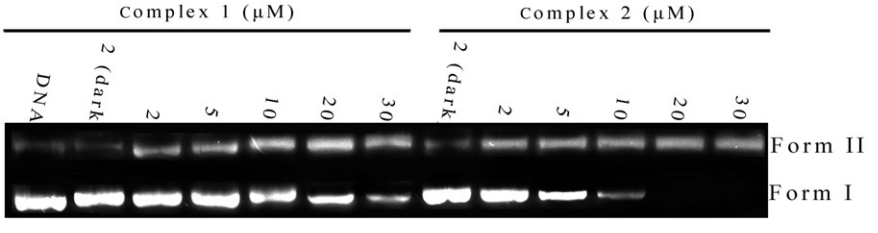

Figure 5. Photoactivated cleavage of pBR322 DNA in the absence and presence of different concentrations of **1** and **2** after irradiation at 365 nm for 1 h.

3.4. *Photoactivated cleavage induced by Ru(II) complexes*

Gel electrophoretic separation showing the cleavage of plasmid pBR322 DNA induced by **1** and **2** is shown in figure 5. The control photoreaction with DNA alone or incubation with the ruthenium complexes in darkness results in little DNA cleavage. With increasing concentrations of the Ru(II) complexes, the amount of Form I gradually diminished, whereas Form II increased, showing the cleavage occurred on one strand. Comparing the cleaving effect of **1** with **2**, complex **2** exhibits more effective DNA cleavage than **1**, consistent with the DNA-binding affinity of the Ru(II) complexes.

3.5. *Cytotoxicity assay* in vitro

The cytotoxicities of **1** and **2** were assessed by MTT toward BEL-7402, HepG-2, and MCF-7 cell lines. In the presence of different concentrations of **1** and **2**, the cells were inhibited; IC_{50} values are listed in table 1. The cell viability is depicted in figure 6. The IC_{50} values for **1** and **2** ranged from 37.96 to 449.22 μmol L^{-1}, suggesting that **1** and **2** exhibit antitumor activity in different degrees. The IC_{50} values show that **2** displays higher cytotoxicity than **1**, but smaller than those of cisplatin. Figure 6 shows cell viability decreased with increasing concentration of complexes.

Table 1. The IC_{50} values for **1** and **2** against selected cell lines.

	IC_{50} (μmol L^{-1})		
Complex	BEL-7402	HepG-2	MCF-7
1	>100	>100	>100
2	44.16	66.35	37.96
Cisplatin	19.32	24.56	12.75

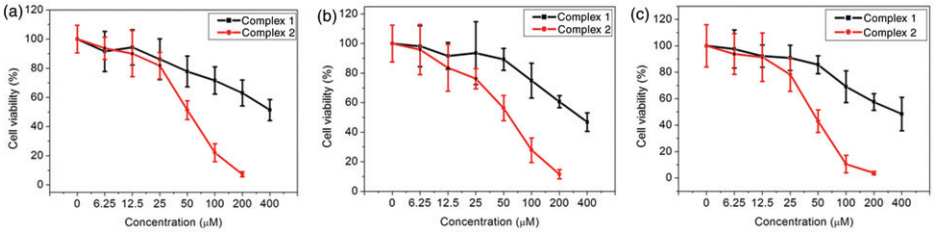

Figure 6. Cell viability of **1** and **2** on tumor BEL-7402 (a), HepG-2 (b), and MCF-7 (c) cell proliferation *in vitro*. Each point is the mean ± standard error obtained from three independent experiments.

3.6. *Apoptosis activity*

In order to gain insight into cell death type induced by **1**, apoptosis assays on BEL-7402 cells were performed with a staining method utilizing AO and EB [23]. AO can pass through cell membrane of living or early apoptotic cells, while staining by EB indicates loss of membrane integrity. Under fluorescence microscope, living cells appear green, necrotic cells stain red but have a nuclear morphology resembling that of viable cells. In the absence of **1**, figure 7(a) shows that the living cells were stained bright green in spots. After treatment with **1** for 48 h, green apoptotic cells containing apoptotic bodies, as well as red necrotic cells, were observed (figure 7b).

3.7. *Antioxidant activity studies*

Activated oxygen has been implicated in tissue damage associated with inflammation, and it has been suggested that hydroxyl radical (•OH) could be a major contributor [27–30]. The hydroxyl radical in aqueous media was generated by the Fenton reaction and antioxidant activities of **1** and **2** against •OH investigated. The suppression ratio for **1** and **2** is listed in table 2. The inhibitory effect of complexes on •OH is depicted in figure 8. The average suppression ratios for •OH increase with increasing concentration of **1** and **2** in the range 0.5–3.5 μmol L^{-1}. The suppression ratio against •OH was 0.39 to 73.93% for **1** and 1.54 to 69.62% for **2**. The antioxidant activity against hydroxyl radical of **1** is higher than that of **2** under identical conditions. The information obtained from this study is helpful to develop new potential antioxidants and new therapeutic reagents for some diseases.

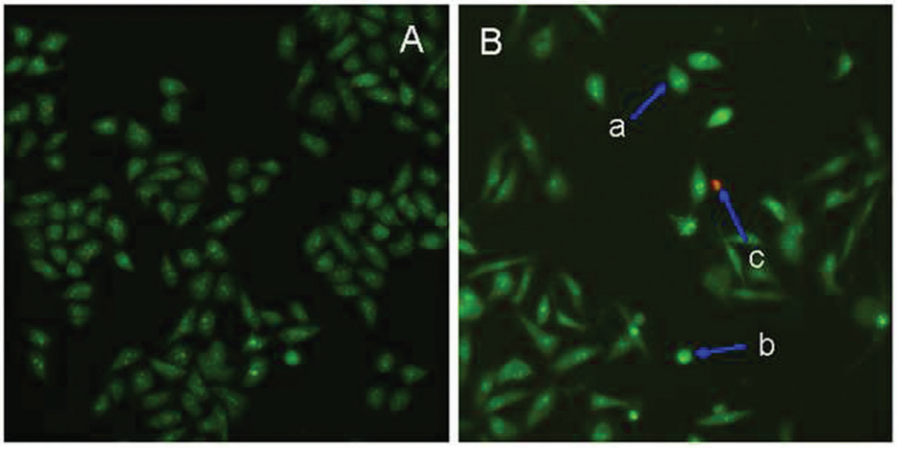

Figure 7. BEL-7402 cell were stained by AO/EB and observed under fluorescence microscopy. BEL-7402 cell without treatment (A) and in the presence of **1** (B) incubated at 37°C and 5% CO_2 for 24 h. Cells in a, b, and c are living, apoptotic, and necrotic cells, respectively.

Table 2. The scavenging ratio (%) of complexes against •OH.

	Average inhibition (%) for •OH						
Complex	0.5	1.0	1.5	2.0	2.5	3.0	3.5 (μmol L^{-1})
1	0.39	8.95	25.29	43.58	68.48	71.60	73.93
2	1.54	8.85	15.77	38.08	48.85	59.23	69.62

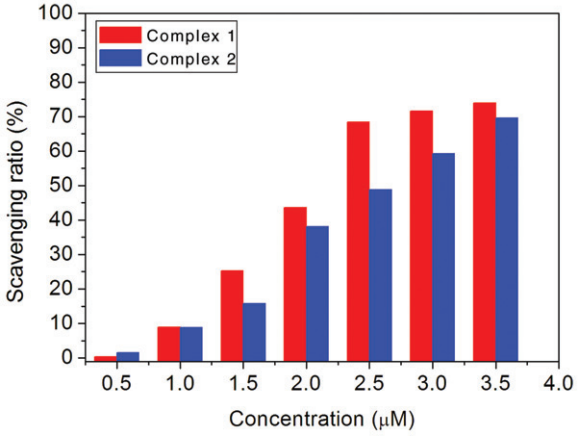

Figure 8. Scavenging effect of **1** and **2** on hydroxyl radicals. Experiments were performed in triplicate.

4. Conclusion

$[Ru(dmp)_2(APIP)]^{2+}$ and $[Ru(dmp)_2(HAPIP)]^{2+}$ have been synthesized and characterized. The DNA-binding behaviors have been investigated by spectroscopic methods,

viscosity measurement, and photocleavage. The results indicate that the two complexes intercalate between DNA base pairs or groove bind. Upon irradiation at 365 nm, **1** and **2** efficiently cleave the plasmid pBR322 DNA. Cytotoxicity assay shows that **2** displays higher cytotoxicity against tumor cells than **1**. Apoptotic studies suggest that **1** can effectively induce apoptosis of BEL-7402 cells. Antioxidant activity experiments show that the two Ru(II) complexes exhibit good antioxidant activity against hydroxyl radical (•OH).

Acknowledgments

This work was supported by the National Nature Science Foundation of China (Nos. 31070858 and 30800227) and Guangdong Pharmaceutical University for financial supports.

References

[1] L.N. Ji, X.H. Zou, J.G. Liu. *Coord. Chem. Rev*., **216–217**, 513 (2001).
[2] F. Gao, H. Chao, F. Zhou, Y.X. Yuan, B. Peng, L.N. Ji. *J. Inorg. Biochem*., **100**, 1487 (2006).
[3] X.C. Yang, Y.N. Liu, S.T. Yao, Y. Xia, Q. Li, W.J. Zheng, L.M. Chen, J. Liu. *J. Coord. Chem*., **64**, 1491 (2011).
[4] K.A. Kumar, K.L. Reddy, S. Satyanarayana. *J. Coord. Chem*., **63**, 3676 (2010).
[5] Y. Liu, Y.J. Liu, J.H. Yao, W.J. Mei, F.H. Wu. *J. Coord. Chem*., **62**, 1701 (2009).
[6] L.F. Tan, F.C. Song, X.Q. Zou, X.L. Ling. *DNA Cell Biol*., **30**, 277 (2011).
[7] K.J. Du, J.Q. Wang, J.F. Kou, G.Y. Li, L.L. Wang, H. Chao, L.N. Ji. *Eur. J. Med. Chem*., **46**, 1056 (2011).
[8] C.P. Tan, S. Hu, J. Liu, L.N. Ji. *Eur. J. Med. Chem*., **46**, 1555 (2011).
[9] U. Schatzschneider, J. Niesel, I. Ott, R. Gust, H. Alborzinia, S. Wölfl. *ChemMedChem*., **3**, 104 (2008).
[10] Y.J. Liu, Z.Z. Li, Z.H. Liang, J.H. Yao, H.L. Huang. *DNA Cell Biol*. DOI:10.1089/dna.2011.1243 (2011).
[11] M.F. Reichmann, S.A. Rice, C.A. Thomas, P. Doty. *J. Am. Chem. Soc*., **76**, 3047 (1954).
[12] M. Yamada, Y. Tanaka, Y. Yoshimoto, S. Kuroda, I. Shimao. *Bull. Chem. Soc. Japan*, **65**, 1006 (1992).
[13] J.B. Chaires, N. Dattagupta, D.M. Crothers. *Biochemistry*, **21**, 3933 (1982).
[14] S. Shi, J. Liu, J. Li, K.C. Zheng, C.P. Tan, L.M. Chen, L.N. Ji. *Dalton Trans*., **1**, 2038 (2005).
[15] Y.J. Liu, Z.H. Liang, Z.Z. Li, J.H. Yao, H.L. Huang. *DNA Cell Biol*. DOI: 10.1089/dna.2010.1170 (2011).
[16] S. Satyanarayana, J.C. Dabroniak, J.B. Chaires. *Biochemistry*, **31**, 9319 (1992).
[17] S. Satyanarayana, J.C. Dabrowiak, J.B. Chaires. *Biochemistry*, **32**, 2573 (1993).
[18] G. Cohen, H. Eisenberg. *Biopolymers*, **8**, 45 (1969).
[19] M.T. Carter, M. Rodriguez, A. Bard. *J. Am. Chem. Soc*., **111**, 8901 (1989).
[20] A. Wolf Jr, G.H. Shimer, T. Meehan. *Biochemistry*, **26**, 6392 (1987).
[21] P. Job. *Ann. Chim. (Paris)*, **9**, 113 (1982).
[22] T. Mosmann. *J. Immunol. Methods*, **65**, 55 (1983).
[23] D.L. Spector, R.D. Goldman, L.A. Leinward. *Cells: A Laboratory Manual*, Vol. 1, Chap. 15, Cold Spring Harbor Laboratory Press, New York, (1998).
[24] C.C. Cheng, S.E. Rokita, C.J. Burrows. *Angew. Chem. Int. Ed. Engl*., **32**, 277 (1993).
[25] F.H. Wu, C.H. Zeng, Y.J. Liu, X.Y. Guan, L.X. He. *J. Coord. Chem*., **62**, 3512 (2009).
[26] D.S. Sigman. *Acc. Chem. Res*., **19**, 180 (1986).
[27] J.M. McCord. *Science*, **185**, 529 (1974).
[28] R.B. Johnston, J.E. Leymeyer. *J. Clin. Invest*., **57**, 836 (1976).
[29] B. Halliwell. *FEBS Lett*., **96**, 238 (1978).
[30] R.A. Greenwald, W.W. Moy. *Arthritis Rheum*., **23**, 455 (1980).